

# Supporting Information

## Fully-Printed All-Solid-State Organic Flexible Artificial Synapse for Neuromorphic Computing

Qingzhou Liu,<sup>1</sup> Yihang Liu,<sup>2</sup> Ji Li,<sup>2</sup> Christian Lau,<sup>1</sup> Fanqi Wu,<sup>1</sup> Anyi Zhang,<sup>1</sup> Zhen Li,<sup>2</sup> Mingrui Chen,<sup>1</sup> Hongyu Fu,<sup>2</sup> Jeffrey T. Draper,<sup>2</sup> Xuan Cao,<sup>\*1</sup> and Chongwu Zhou<sup>\*1, 2</sup>

<sup>1</sup> Mork Family Department of Chemical Engineering and Materials Science and <sup>2</sup> Ming Hsieh Department of Electrical Engineering, University of Southern California, Los Angeles, California 90089, United States.

\* To whom correspondence should be addressed. E-mail: [caoxuan1234@gmail.com](mailto:caoxuan1234@gmail.com) and [chongwuz@usc.edu](mailto:chongwuz@usc.edu).

Q. Liu and Y. Liu contributed equally.

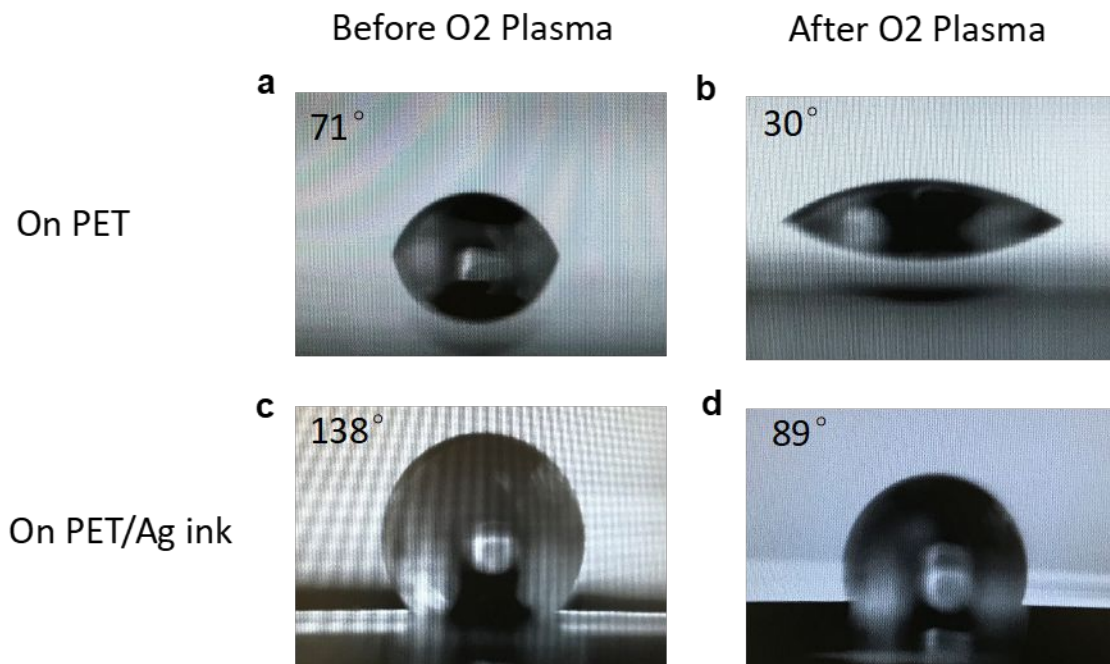


**Figure S1.** Surface modification with oxygen plasma. Contact angles of water on unmodified PET substrate (a), on oxygen plasma-modified PET (b), on unmodified silver conductive film (c), and on oxygen plasma-modified silver conductive film (d). After being treated with oxygen plasma (100 W, 150 mTorr) for 30 seconds, the contact angle of water changes from 71° to 30° on PET substrate, and from 138° to 89° on silver film, which indicates the surface of both PET and silver film become more hydrophilic.

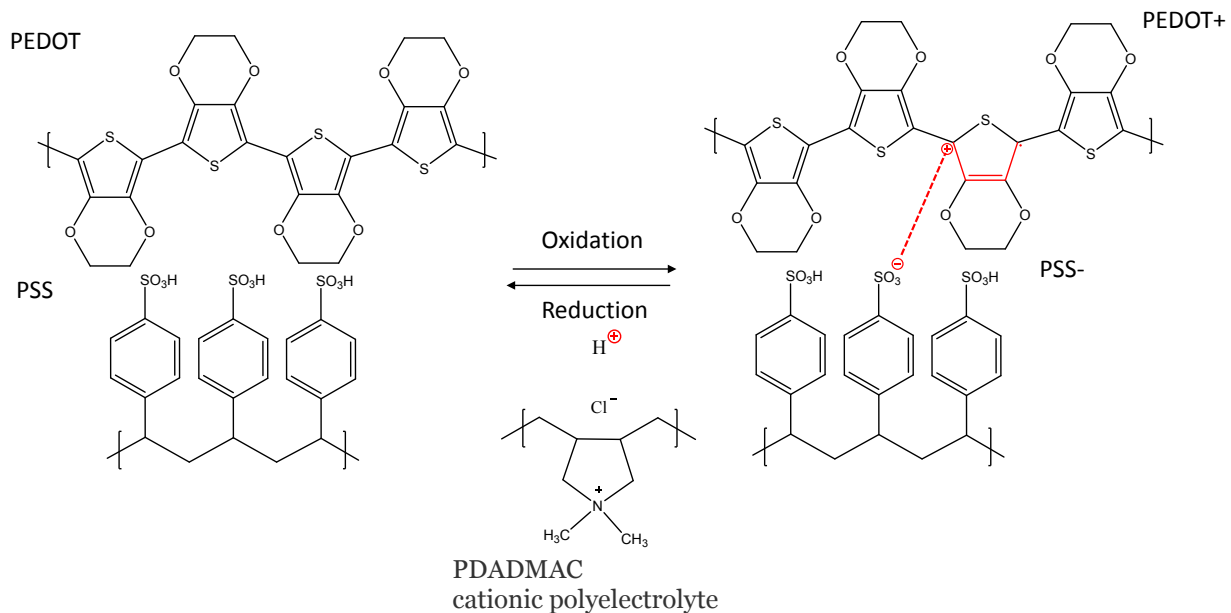


**Figure S2.** Oxidation and reduction reaction of an PEDOT:PSS based all-solid organic neuromorphic devices. The molecular structures of PEDOT:PSS and PDADMAC are illustrated in this figure. Upon applying a negative  $V_{pre}$  to the PEDOT:PSS electrode, protons flow from the postsynaptic electrode into the presynaptic electrode through PDADMAC electrolyte, resulting in deprotonation of the PEI, and further cause the oxidation of PEDOT due to charge neutrality. This causes holes to be generated on the PEDOT backbone, thereby reducing the electronic resistivity of the postsynaptic electrode. The reaction is reversed when applying a positive presynaptic potential. The charge transfer is marked in red in the figure.

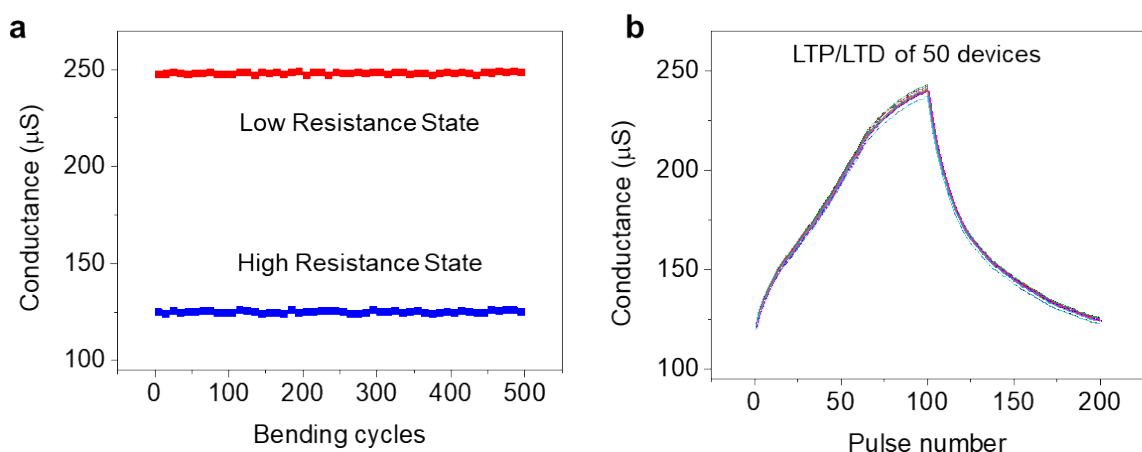


**Figure S3.** Flexibility and uniformity study. (a) Electrical stability of neuromorphic devices under 500 mechanical bending cycles. In this measurement, the sample was bent with a radius of curvature of 10 mm for 100 cycles. Each bending cycle included one compression and one extension of the functional film. After every 5 bending cycles, positive and negative pulses were applied to measure the electrical properties of the device. The low- and the high-resistance states were recorded, respectively. This result shows that the flexible artificial synapse exhibits outstanding mechanical deformation endurance. (b) LTP and LTD were performed on 50 devices with same geometry. For each measurement, 100 positive pulses followed with 100 negative pulses were applied to each device and the conductance was recorded. The results show the good uniformity of our devices and demonstrate the reliability of using printing to fabricate such neuromorphic devices.

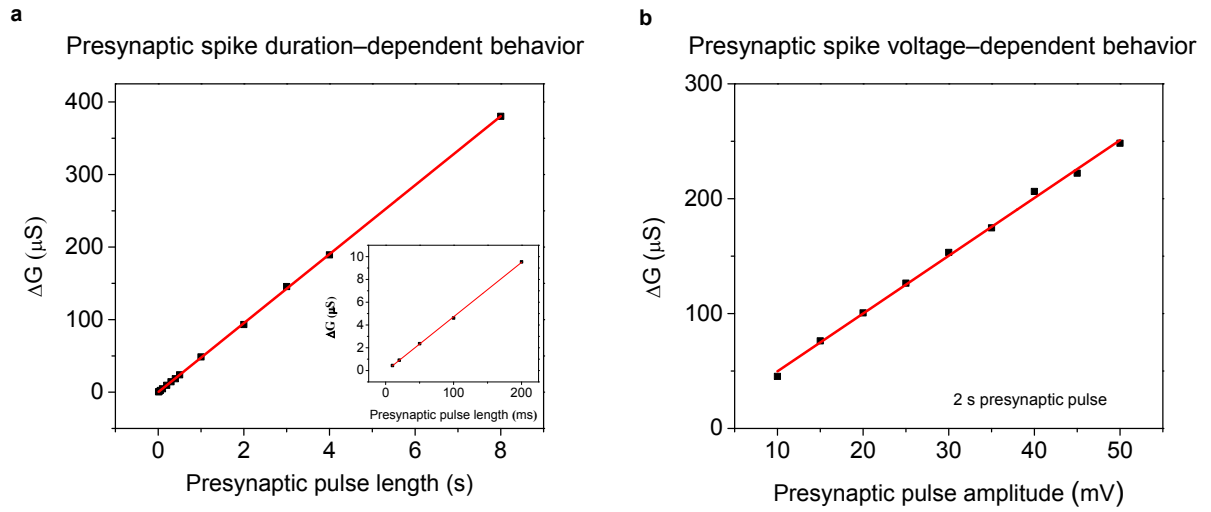


**Figure S4.** Change in postsynaptic conductance as a function of presynaptic pulse duration (a) and amplitude (b). The measured excitatory post-synaptic currents (EPSC) are converted into conductance change ( $\Delta G$ ) of the post-synaptic electrode. With the presynaptic voltage fixed at 20 mV, the  $\Delta G$  values increases from 0.5  $\mu S$  (inset) to 371  $\mu S$  for spike duration ranges from 10 ms to 8 s, respectively. The spike voltage-dependent EPSCs are also studied. With the presynaptic pulse duration fixed at 2 s, the  $\Delta G$  increases from 48  $\mu S$  to 251  $\mu S$  for spike voltage ranges from 10 mV to 50 mV. As the linear fitting shown in both figures (in red), the conductance change is a linear function of presynaptic pulse duration and voltage.

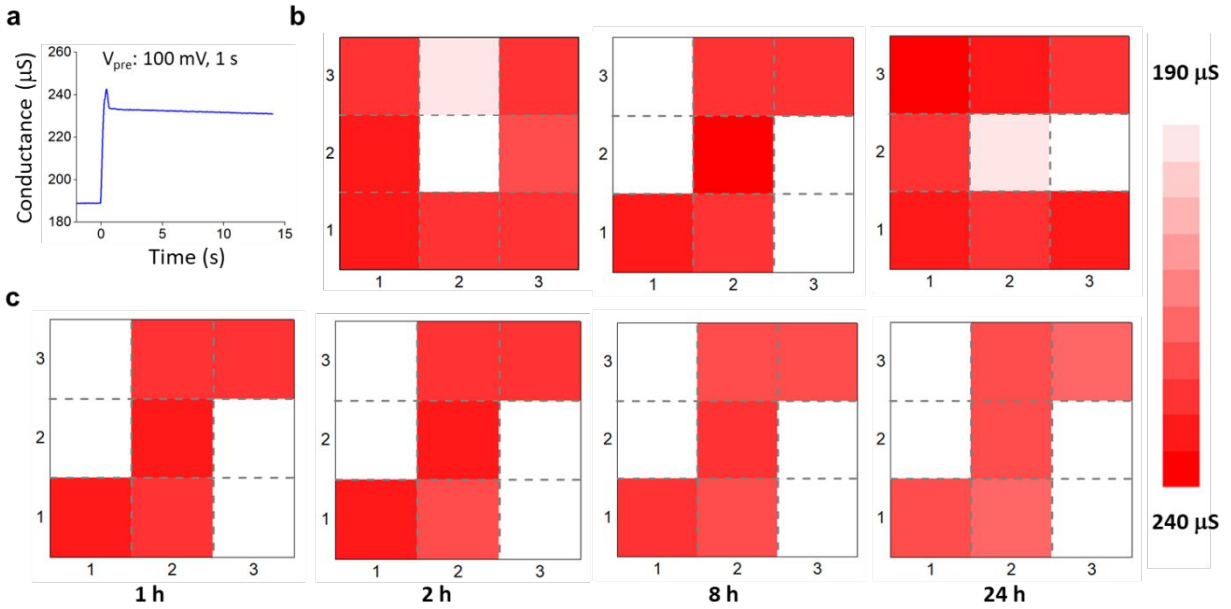


**Figure S5.** Dynamic image processes and retention. (a) Functionality test on an organic synaptic transistor. As the presynaptic input arrived at 0 s, the conductance (synaptic weight) changes from low conductance state ( $\sim 190 \mu\text{S}$ ) to high conductance state ( $\sim 230 \mu\text{S}$ ). (b) Dynamic image processes on a  $3 \times 3$  synaptic array with local presynaptic input. The diagram shows that the capital letter “U”, “S”, and “C” were memorized by the synaptic array. (c) Retention (forgetting) evaluation of the capital letter “S” after 1, 2, 8 and 24 hours after the image was memorized by the synaptic array.

**Table S1.** Parameters of datasets and neural networks

Dataset	Input size	Training examples	Testing examples	Neural network configuration	Application
ORL	23x28	240	160	644x100x40	Face recognition
Optical Recognition of Handwritten Digits	8x8	3823	1797	64x50x10	Digit recognition
MNIST	28x28	50000	10000	784x300x10	Digit recognition